© 2020. Published by The Company of Biologists Ltd | Journal of Cell Science (2020) 133, jcs243931. doi:10.1242/jcs.243931

RESEARCH ARTICLE

Evidence for macromolecular crowding as a direct apoptotic stimulus

Priyanka S. Rana, Manabu Kurokawa and Michael A. Model*

ABSTRACT

Potassium loss and persistent shrinkage have both been implicated in apoptosis but their relationship and respective roles remain controversial. We approached this problem by clamping intracellular sodium and potassium in HeLa or MDCK cells using a combination of ionophores. Although ionophore treatment caused significant cell swelling, the initial volume could be restored and further reduced by application of sucrose. The swollen cells treated with ionophores remained viable for at least 8 h without any signs of apoptosis. Application of sucrose and the resulting shrinkage caused volume-dependent intrinsic apoptosis with all its classical features: inversion of phosphatidylserine, caspase activation and Bcl-2-dependent release of cytochrome *c* from mitochondria. In other experiments, apoptosis was induced by addition of the protein kinase inhibitor staurosporine at various degrees of swelling. Our results show that: (1) persistent shrinkage can cause apoptosis regardless of intracellular sodium or potassium composition or of the state of actin cytoskeleton; (2) strong potassium dependence of caspase activation is only observed in swollen cells with a reduced density of cytosolic proteins. We conclude that macromolecular crowding can be an important factor in determining the transition of cells to apoptosis.

KEY WORDS: Apoptosis, Cell volume, Hyperosmotic stress, Macromolecular crowding, K^+, Volume sensing

INTRODUCTION

Osmotic swelling and shrinkage are a common occurrence in the life of the cell. This is true not only for simple organisms that have no control over their environment, but for mammalian cells as well. Oral and esophageal endothelial cells, medullary parts of nephrons, blood cells, lymphoid tissues and skeletal muscles can all be subject to osmotic stress.

Because mammalian cells lack a stiff and water-impermeable wall, any changes in osmolarity would inevitably result in volume changes due to an influx or efflux of water. This stimulates a host of cellular reactions involving secondary messengers, free radicals, pH changes, phosphorylation, enzyme activity and other factors that operate downstream of volume changes (Burg et al., 2007). However, despite a long-standing interest, the nature of the primary volume sensor – the first responder to swelling or shrinkage – remains unknown (Burg, 2000; Mongin and Orlov, 2001; Papakonstanti et al., 2000; Hoffmann et al., 2009; Koivusalo et al., 2009; Pedersen et al., 2011). It stands to reason that the initial sensor of cell volume must be some aspect of the volume itself: a change in size, surface area, concentration, proximity between molecules or mechanical forces directly resulting from changes in cell size. Of such processes, the following have received most attention in the literature.

(1) Signaling through cell size (in a general and undefined sense). Although growing and dividing cells maintain their average size and must be able to measure it somehow, the molecular mechanisms relating their size to signaling remain highly speculative (Marshall, 2016).

(2) Signaling through membrane tension. Stretching of the lipid bilayer during swelling can activate mechanosensitive ion channels (Janmey and Kinnunen, 2006). However, lateral compression of lipids during shrinkage seems unlikely due to flexibility of the membrane.

(3) Signaling through the cytoskeleton. Owing to its relative stiffness and numerous interconnected parts, the cytoskeleton can be strongly affected by changes in cell shape and volume. Assembly and disassembly of actin microfilaments regulate numerous membrane channels, transporters, receptors and cytoplasmic signaling proteins (Papakonstanti et al., 2000; Zigmond, 1996; Pedersen et al., 2001).

(4) Signaling through concentrations of ions. Accumulation or loss of water would automatically change the concentrations of all membrane-impermeant chemicals. If a cell shrinks by 30%, for example, the intracellular concentrations will increase by 43% or even more (since water occupies only a part of cell volume). Monovalent ions are often seen as the main candidates for the role of volume sensor as they are known to affect many cellular reactions (Orlov and Hamet, 2006; Klimanova et al., 2019) and their concentrations are maintained relatively stable under normal conditions.

(5) Signaling through the density of macromolecules (macromolecular crowding). The very high density of macromolecules in the cytosol and in organelles creates a rather special environment. At such high concentrations, thermodynamic activity of proteins (their 'effective concentration') shows a nonlinear dependence on the mass/volume concentration, so that even a minor shrinkage or swelling can produce a greatly amplified effect. The best-studied consequences of macromolecular crowding relate to protein stability and reaction kinetics (Minton, 2001; Gnutt and Ebbinghaus, 2016; Mittal et al., 2015; Mourão et al., 2014). In the previous example of a 30% shrinkage, the activity of proteins could increase not by 43% but by a much larger factor, causing oligomerization of proteins and acceleration of reactions, perhaps by orders of magnitude. The other, possibly significant, factor is the proximity of proteins to water molecules, causing changes in the physicochemical properties of water (Fulton, 1982; Garner and Burg, 1994).

Although macromolecular crowding has been extensively studied *in vitro*, its implications for living cells remain poorly understood.

Department of Biological Sciences, Kent State University, Kent, OH 44242, USA.

*Author for correspondence (mmodel@kent.edu)

M.A.M., 0000-0002-3292-3382

Handling Editor: John Heath
Received 14 January 2020; Accepted 13 March 2020

Journal of Cell Science (2020) 133, jcs243931. doi:10.1242/jcs.243931

The simplest, and sometimes the only practical way to experimentally manipulate macromolecular crowding is to put cells into an anisosmotic solution or to upset ion balance by altering membrane permeability or the ionic composition of the medium (Maeno et al., 2006a,b). However, such manipulations are liable to produce side effects by altering membrane and/or cytoskeletal tension as well as redistributing monovalent ions. Thus, it is risky to ascribe any swelling- or shrinkage-induced response to macromolecular crowding before ruling out more conventional explanations. In discussing the nature of signaling by cell volume, the authors of one comprehensive review (Hoffmann et al., 2009) dismiss the effects of macromolecular crowding as lacking experimental evidence in cells other than erythrocytes (Colclasure and Parker, 1991, 1992). Yet, alterations of molecular properties upon changes in macromolecular density are so numerous and well documented that it is hard to imagine why living cells should be exempt from such effects; indeed, the idea that macromolecular crowding may act as a primary sensor of cell volume is never far away (Alfiery and Petronini, 2007; Al-Habori, 2001; Ghosh et al., 2007; Garner and Burg, 1994; Burg, 2000; Orlov et al., 2018; Zhou et al., 2008; Hoffmann and Pedersen, 2011).

Apoptotic cell death provides an important and relevant example. Apoptosis is a form of programmed cell death executed by activation of the caspase family of cysteine proteases. Apoptosis can be induced by genotoxic or cytotoxic stress (such as inhibition of essential enzymes, oxidative damage, starvation or heat) through the so-called intrinsic or mitochondrial pathway. This pathway is characterized by permeabilization and depolarization of the outer mitochondrial membrane and the release of cytochrome *c* from the intermembrane space into the cytosol under the control of pro-apoptotic and anti-apoptotic Bcl-2 (also known as apoptosis regulator Bcl-2) family proteins (Elmore, 2007). Once released from the mitochondria, cytochrome *c* activates an adaptor protein, APAF1, which in turns activates caspase-9.

Shrinkage and apoptosis are interrelated in at least two ways. First, in addition to the above-mentioned reactions, apoptosis induced by almost any stimulus causes cell shrinkage and a loss of water (termed apoptotic volume decrease or AVD). AVD may be a consequence of the activation of potassium channels and efflux of potassium and chloride: stimulation of apoptosis in the presence of potassium or chloride blockers often abrogates all other manifestations of apoptosis (Bortner and Cidlowski, 1998, 2004). This suggests that either loss of potassium or some other aspect of shrinkage is required for development of apoptosis (Bortner and Cidlowski, 2004; Bortner and Cidlowski, 2007; Yu et al., 2001; Park and Kim, 2002).

Second, persistent hyperosmotic shrinkage also causes apoptosis (Bortner and Cidlowski, 1996; Horio et al., 2001; Friis et al., 2005; Maeno et al., 2006a,b; Burgos et al., 2019; Michea et al., 2000; Luo et al., 2007; Ernest et al., 2008; Shimizu et al., 2007). Many cell types, when exposed to hyperosmotic solutions, gradually restore their volume through a process known as regulatory volume increase (RVI). RVI is mediated by an increase in sodium and chloride permeability through Na^+-K^+-$2Cl^-$ cotransporter, Na^+-H^+ exchanger and Cl^--HCO_3^- exchanger (Mongin and Orlov, 2001). Cells that are able to recover their volume through RVI survive hypertonic shock, but those incapable of RVI proceed to apoptotic death (Bortner and Cidlowski, 1996; Ernest et al., 2008). In the case of hyperosmotic apoptosis, potassium loss is clearly secondary to shrinkage (the immediate effect would be a concentration increase rather than a decrease); thus, its significance is unclear. In one study, an increase in potassium permeability has been detected in fibroblasts after exposure to a hyperosmotic solution but caused no overall loss of intracellular potassium (Friis et al., 2005). Other authors have induced hyperosmotic apoptosis in a high-potassium medium that was expected to prevent any loss of intracellular potassium (Ghosh et al., 2007). It has been proposed that protein density is better suited for the role of shrinkage sensor (Friis et al., 2005; Ernest et al., 2008; Maeno et al., 2006a,b).

In the present work, we took a more direct approach to the problem. We used a combination of ionophores (valinomycin, nigericin, gramicidin) with simultaneous inhibition of the Na^+-K^+ pump by ouabain; this treatment has proved to be effective in equilibrating intracellular and extracellular potassium (Rana et al., 2019). Exposure to ionophores caused cell swelling, but the cells remained viable with no signs of apoptosis developing for at least 8 h. By adding membrane-impermeant sucrose at various concentrations and/or the actin-disrupting drug cytochalasin D simultaneously with ionophores, we were able to control intracellular ions and cell density independently. In other experiments, we applied a chemical inducer of apoptosis, the protein kinase inhibitor staurosporine (ST), together with ionophores. Our results led us to conclude that shrinkage can stimulate apoptosis at any monovalent ion composition and acts, most likely, through an increase in macromolecular crowding. Potassium does play a role, albeit a smaller one that is mostly limited to swollen cells.

RESULTS

Sucrose increases macromolecular density in VNGO-treated cells

Osmotic shrinkage of intact cells affects the intracellular concentration of monovalent ions, which complicates interpretation of experiments testing the effects of shrinkage. Therefore, we fixed intracellular ion concentrations by exposing cells to a cocktail of valinomycin, nigericin and gramicidin ionophores (VNG) and a Na^+-K^+ pump inhibitor ouabain (O). We have previously shown that this treatment is the most effective for equalizing intracellular and extracellular potassium levels (Rana et al., 2019).

HeLa cells exposed to VNGO responded with significant swelling. Inclusion of 50 mM sucrose in the buffer restored the initial cell volume, and higher sucrose concentrations changed swelling to shrinkage (Fig. 1A,C,D). Macromolecular densities changed correspondingly, from 220 mg/ml in DMEM to 300 mg/ml in 100 mg/ml sucrose. These densities remained stable, at least between 1 h and 6 h of incubation (Fig. 1B).

Shrinkage in VNGO-treated cells activates apoptotic markers

Cells swollen by permeabilization with VNGO remained viable for at least 8 h without developing any signs of apoptosis. However, the presence of sucrose in the buffer strongly upregulated all of the tested apoptotic markers: caspase staining, annexin V binding and cytochrome *c* release.

Fig. 2 shows the results of caspase staining experiments. Very few caspase-positive cells were observed in the cells swollen by VNGO; however, the presence of sucrose in the buffer dramatically stimulated apoptosis. Positive NucView staining (indicating caspase-3 activity) was observed in roughly half of the cells in 100 mM sucrose. Apoptosis in MDCK was more prominent in high-sodium buffer (HSB) compared to that in high-potassium buffer (HPB) (P=0.001), whereas the effect of ion composition on caspase activation in HeLa cells was barely noticeable (P=0.1 for 100 mM sucrose), except in 75 mM sucrose. Similar results were obtained in a single experiment with Madin–Darby bovine kidney cells (MDBK; not shown).

Journal of Cell Science (2020) 133, jcs243931. doi:10.1242/jcs.243931

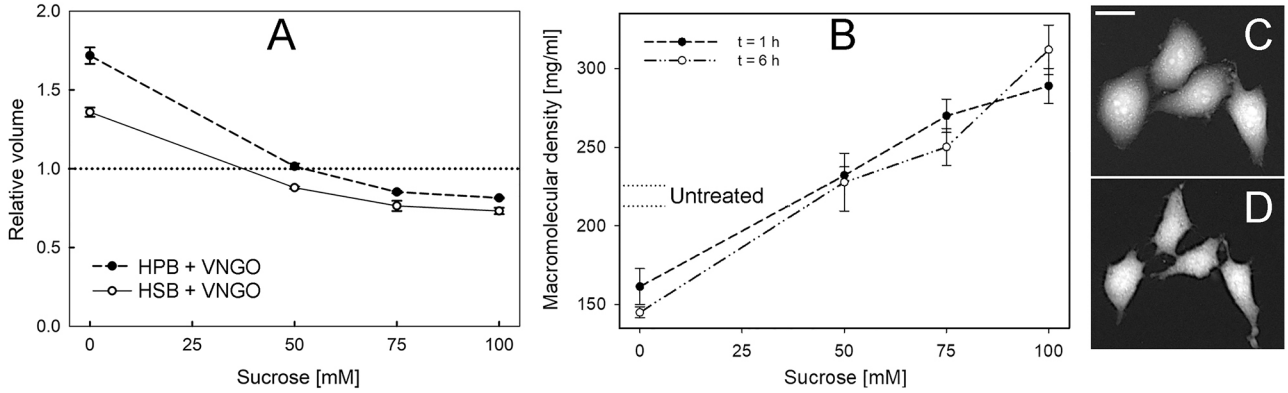

Fig. 1. Changes in volume and macromolecular density in VNGO-treated HeLa cells. (A) Changes in the volumes of adherent HeLa cells after a 60 min incubation in HPB containing VNGO or in HSB containing VNGO, with the addition of different concentrations of sucrose. The volumes are shown relative to pretreatment volumes in DMEM (horizontal dotted line). The results represent 10–27 cells per treatment in a single experiment. Similar data have been published previously (Rana et al., 2019). Longer incubation times did not cause major changes in cell volumes. (B) Changes in macromolecular density after 1 h and 6 h in HPB containing VNGO with the addition of different concentrations of sucrose. The range (mean±s.e.m.) for the same cells in DMEM before treatment (92 cells) is indicated with horizontal dotted lines. For every treatment condition, 20–26 cells were analyzed. (C,D) TTD images of cells before (C) and after (D) 6 h incubation in HPB containing VNGO with 100 mM sucrose. The intensities are displayed on a logarithmic scale, where local brightness is proportional to cell thickness. Scale bar: 20 µm.

Phosphatidylserine translocation in MDCK cells displayed similar dependence on sucrose (Fig. 3). As with caspase in MDCK, a slightly higher percentage of annexin-positive cells (indicating the presence of phosphatidylserine on the cell surface) was observed in HSB than in HPB (P=0.008 for 100 mM sucrose), but the effect of sucrose concentration was much stronger. We further measured cytochrome *c* release from HeLa cells (Fig. 4). In this case, a slightly higher percentage of apoptotic cells was observed in HPB than in HSB (P=0.075 for 100 mM sucrose and P=0.0006 for 75 mM sucrose) but, as in other cases, the effect of sucrose concentration was much more prominent. Sucrose at 75 mM or higher caused cytochrome *c* release in 70–97% of HeLa cells, whereas in the absence of sucrose only 1.5–2.0% of cells were affected.

Bcl-2 overexpression inhibits the release of cytochrome *c* from mitochondria in shrunken HeLa cells

The effect of Bcl-2 overexpression on apoptosis was investigated in HeLa cells in which apoptosis was stimulated by an 8 h incubation in HPB containing VNGO and 100 mM sucrose. Bcl-2 was overexpressed as a GFP–Bcl-2 fusion protein and expression was assessed visually using fluorescence microscopy.

As expected, Bcl-2 proteins suppressed the release of cytochrome *c* from mitochondria. Of 215 cells in the GFP–Bcl-2-transfected sample, 72% overexpressed Bcl-2 and only 18% released cytochrome *c*. By contrast, of 144 untransfected cells, 89% underwent apoptosis (Fig. 5). The prevalence of cytochrome *c* release among Bcl-2-positive and Bcl-2-negative cells within the

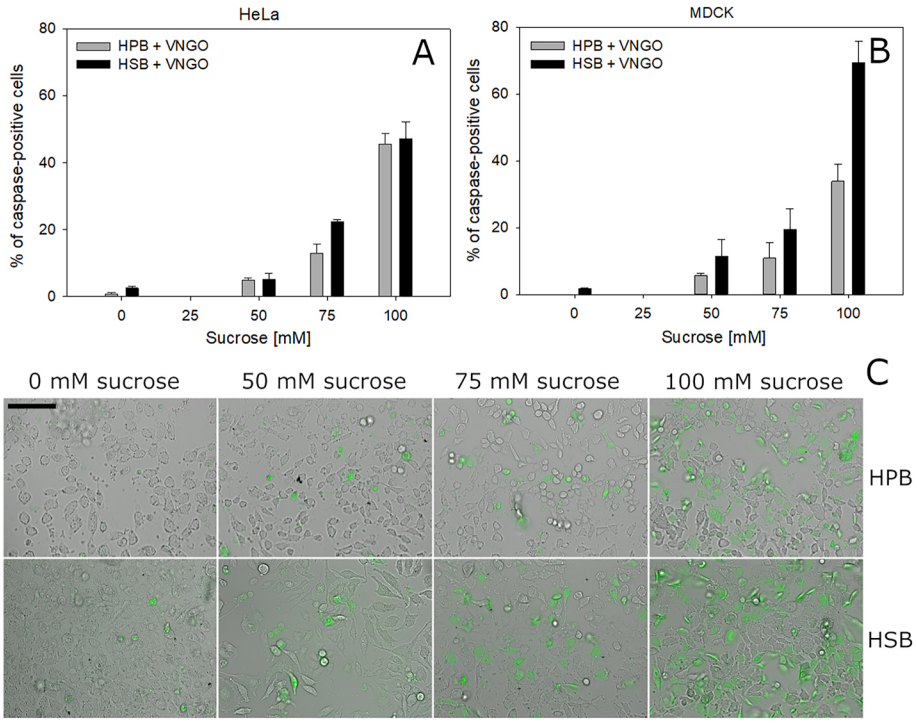

Fig. 2. Caspase-3 activation in cells treated with VNGO in HPB or HSB in the presence of various sucrose concentrations. (A,B) Percentage of caspase-positive HeLa and MDCK cells post-treatment. Bars represent mean±s.e.m. of n=2 (for 75 mM sucrose) or n=5 (for all other treatments) experiments. (C) Overlay of brightfield images of HeLa cells and NucView 488 fluorescence (green), indicating caspase-3 activation. Scale bar: 100 µm.

Journal of Cell Science (2020) 133, jcs243931. doi:10.1242/jcs.243931

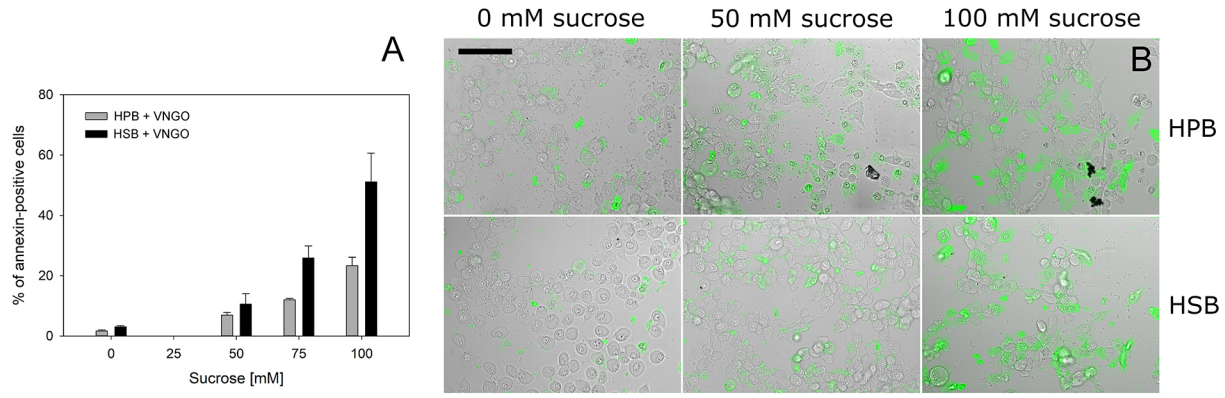

Fig. 3. Phosphatidylserine translocation in MDCK cells treated with VNGO in HPB or HSB in the presence of various sucrose concentrations. (A) Percentage of annexin-positive MDCK cells (*n*=3). (B) An overlay of fluorescence and brightfield images of MDCK cells stained with Annexin V-FITC (green channel). Scale bar: 100 µm.

transfected sample was not determined. These results confirm that cells subjected to shrinkage display the normal features of mitochondrial apoptosis.

Apoptotic sensitivity to potassium depends on VNGO induced swelling

We also wished to know whether the presence of potassium had any inhibitory effect on apoptosis in cells that were either swollen or kept at their normal volume. However, since very little apoptosis developed under these conditions, the experiment had to be modified. We thus switched to a different apoptotic model, where apoptosis in HeLa cells was induced by the protein kinase inhibitor ST (Bertrand et al., 1994; Koh et al., 1995; Model et al., 2018). ST was applied for 8 h in HPB, HSB, and in similar buffers with intermediate potassium concentrations. Because these experiments were carried out in simple buffers rather than full culture medium, we first verified that such a substitution had no major effect on the potency of ST to stimulate apoptosis (not shown).

Next, ST was applied under conditions that otherwise produced only few apoptotic cells: HPB containing VNGO and either 0 mM or 50 mM sucrose. In the cells swollen in the absence of sucrose, caspase activation was strongly inhibited by potassium: as little as 5 mM K^+ reduced caspase activation by a half (Fig. 6). However, restoration of the initial cell volume by the addition of 50 mM sucrose eliminated the effect of potassium on caspase activation. We did not test higher sucrose concentrations in the presence of ST because under such conditions apoptosis would have resulted from the combined effects of ST and shrinkage.

Inhibition of actin polymerization by cytochalasin D had no effect on caspase activity

Having eliminated potassium as an apoptotic stimulus in shrunken cells, we tested whether the actin cytoskeleton plays any active role in shrinkage- or ST-induced apoptosis. Depolymerization of the actin cytoskeleton by cytochalasin D did not prevent caspase activation in apoptosis induced by either factor (Fig. 7).

DISCUSSION

Our main goal was to obtain a better insight into the nature of the initial apoptotic trigger in shrinkage-induced apoptosis. Unfortunately, since protein density cannot be manipulated by genetic engineering or by specific inhibitors, many of the standard biological approaches cannot be applied to investigate the effects of crowding; they have to be surmised by exclusion of other possible explanations or by simulating similar effects in a test tube. While the latter remains a task for the future, in this work we have adopted a ‘proof by contradiction’ approach. It is certainly impossible to eliminate every alternative, and we have focused on the two other aspects of cell volume that might in principle initiate downstream signaling for apoptosis: potassium depletion and cytoskeleton-

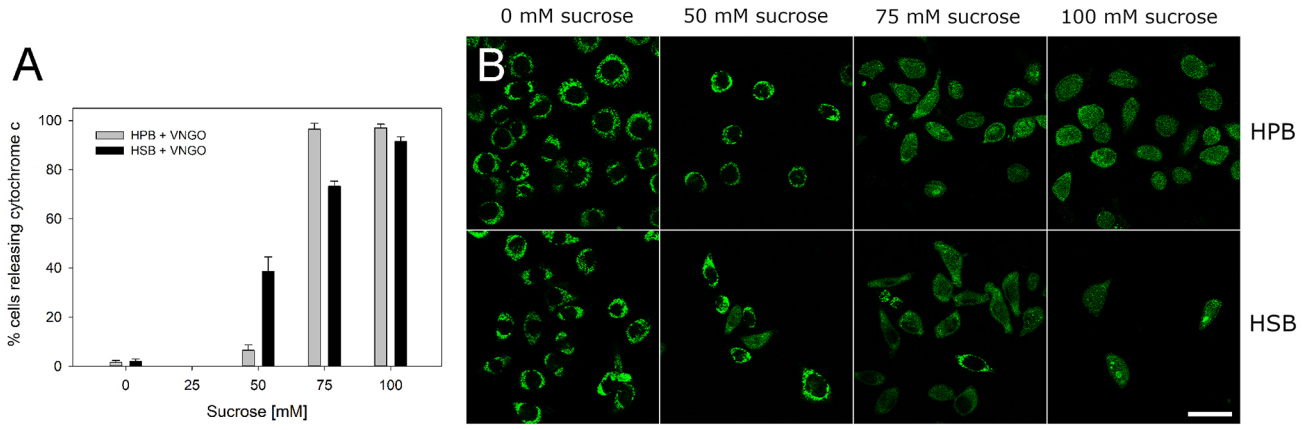

Fig. 4. Cytochrome *c* release in HeLa cells treated with VNGO in HPB or HSB in the presence of various sucrose concentrations. (A) Percentage of apoptotic HeLa cells, as reported by cytochrome *c* release. Cells with uniform and nuclear staining were counted as positive (*n*=4). (B) Cytochrome *c* fluorescence immunostaining. Scale bar: 50 µm.

Journal of Cell Science (2020) 133, jcs243931. doi:10.1242/jcs.243931

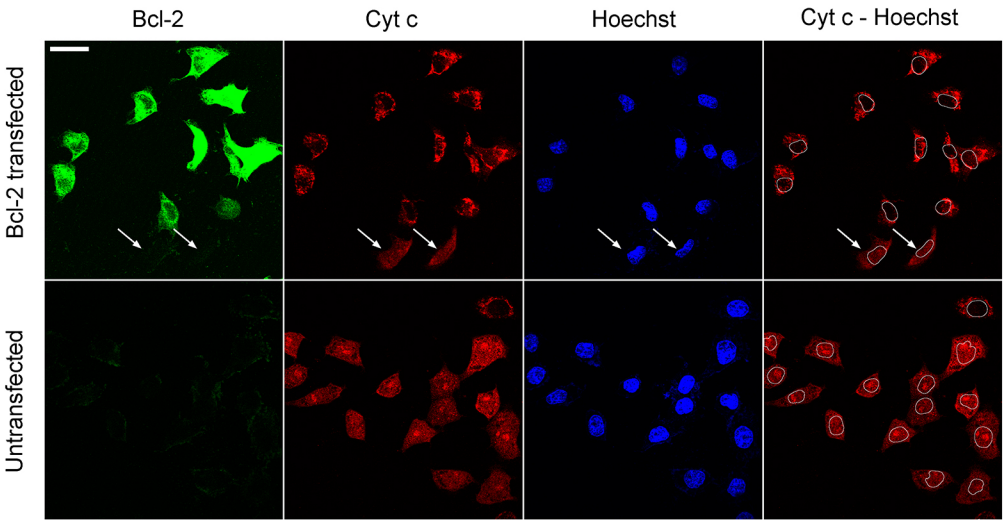

Fig. 5. Expression of anti-apoptotic Bcl-2 inhibits cytochrome *c* release in HeLa cells exposed to HPB containing VNGO and 100 mM sucrose. GFP–Bcl-2 is shown in green, cytochrome *c* staining is shown in red and Hoechst staining is shown in blue. The two arrows in the GFP–Bcl-2 transfected sample point to cells that failed to express Bcl-2; those cells underwent apoptosis. Images on the right show the boundary of the nucleus overlaid on the cytochrome *c* image. The boundaries were created by applying a median filter to images of Hoechst staining, segmenting the nuclei by intensity threshold and making outlines in ImageJ. Scale bar: 25 µm.

mediated effects (Mechanisms 3 and 4 listed in the Introduction). Tension in the lipid bilayer with activation of stretch-sensitive anion channels (Strange et al., 2019) would have been an additional possibility if the cells underwent swelling instead of shrinkage; however, under conditions of shrinkage, it is less likely to be a factor. Although one can imagine a healthy cell displaying an intermediate level of membrane stretch that increases during swelling and decreases during shrinkage, we are not aware of any experimental support for such a scenario.

Fig. 8 illustrates our working model. Although potassium loss cannot be an immediate consequence of shrinkage (the immediate consequence would rather be a concentration increase), it might still occur at a later stage (Friis et al., 2005). The interplay between potassium depletion and apoptotic shrinkage has been a much-discussed topic, and therefore we have examined their respective roles. In effect, we used hyperosmotic apoptosis as a tool to investigate the general relationship between protein density, potassium, and the cytoskeleton in apoptosis.

Our experimental approach was based on the previous finding that treatment with VNGO results in the most thorough cell depolarization and equilibration of potassium between internal and external pools; all other combinations of ionophores and/or ouabain

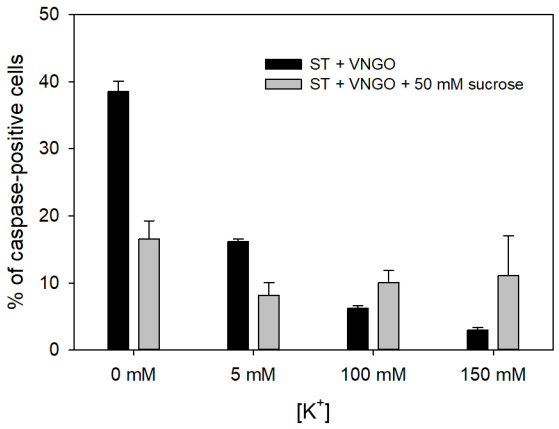

Fig. 6. Caspase activity during ST-induced apoptosis in HeLa cells was sensitive to potassium concentration only when the cells were swollen in VNGO. Apoptotic sensitivity to potassium was lost when the initial volume was restored by addition of 50 mM sucrose. The experiment was repeated in triplicate, and a total of 636–1464 cells were analyzed for each condition.

tested were less effective (Rana et al., 2019). HeLa, MDCK, and MDBK cells (the results with the latter were not included), but not SH-SY5Y cells, remained viable and excluded not only Acid Blue 9, but also Trypan Blue and fluorescent dextran (not shown) after prolonged exposure to VNGO in HEPES-buffered solutions. Gramicidin treatment alone caused swelling and extensive apoptosis after 8 h, but valinomycin treatment did not, and moreover, partly suppressed apoptosis when applied together with gramicidin (not shown). This result is at variance with previous reports, where valinomycin was found to stimulate apoptosis (Inai et al., 1997; Furlong et al., 1998; Abdalah et al., 2006) and gramicidin caused necrosis (David and Rajasekaran, 2015). However, as we have established in earlier trials, VNGO did indeed cause massive cell death when applied in full growth medium (DMEM containing FBS); this may explain the difference between our results and the cited studies. Prevention of apoptosis in the buffer by valinomycin is interesting and deserves further investigation.

Although cells swollen by exposure to VNGO remained viable, osmotic shrinkage by sucrose produced apoptosis. Apoptosis was verified by assaying caspase activation, cytochrome *c* release from mitochondria and inversion of phosphatidylserine. Valinomycin is known to depolarize mitochondria directly (Furlong et al., 1998), and therefore mitochondrial depolarization could not be used as an apoptotic marker. Hoechst staining of DNA in apoptotic cells was brighter than in unaffected cells but did not show the characteristic chromatin condensation, so it was not used for the identification of apoptotic cells. Overexpression of Bcl-2 suppressed cytochrome *c* release, confirming that apoptosis was of the intrinsic type (Criollo et al., 2007).

Apoptosis strongly depended on the amount of sucrose added: it was negligible in swollen cells without sucrose and reached 50% or more when 150 mM sucrose was present. Because potassium depletion is often seen as an essential feature of apoptosis (Kunzelmann, 2016; Yu, 2003; Park and Kim, 2002), we investigated the effect of ion composition. We found that sucrose-induced shrinkage produced apoptosis both in HPB and HSB. The effect of potassium-for-sodium substitution on the development of apoptotic markers was minor and sometimes inconsistent in HeLa (as in Fig. 4A), and although the effect was more pronounced in MDCK cells, it was still much weaker than the effect of shrinkage. To investigate further, we induced apoptosis using the protein kinase inhibitor ST in cells that were either swollen in VNGO or

Journal of Cell Science (2020) 133, jcs243931. doi:10.1242/jcs.243931

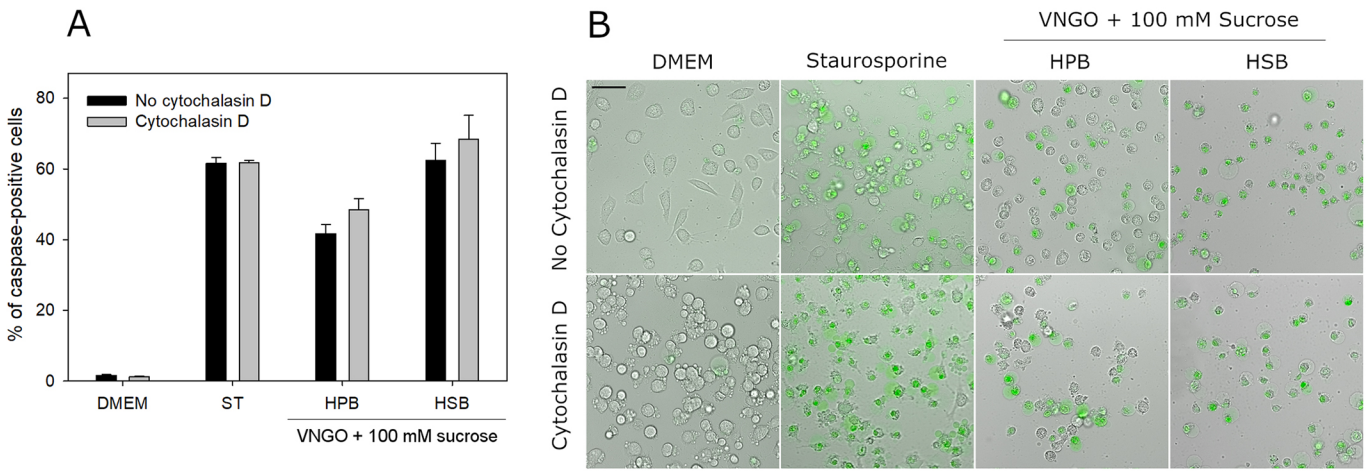

Fig. 7. Addition of cytochalasin D has no effect on caspase activation in ST- and shrinkage-induced apoptosis. (A) Percentage of caspase-positive cells in the presence and absence of cytochalasin D during treatment with ST or VNGO and 100 mM sucrose (between 98 and 621 cells analyzed per treatment; *n*=3). (B) The lack of effect of cytochalasin D on caspase activation in ST- and shrinkage-induced apoptosis in HeLa cells. Overlays of brightfield images and NucView 488 fluorescence (green; indicating caspase-3 activation) are shown. Scale bar: 50 µm.

restored approximately to their resting volume by addition of 50 mM sucrose; in the absence of ST, there was little apoptosis under these conditions. Strong inhibition of caspase activation by as little as 5 mM potassium was observed in swollen cells. However, the effect of potassium was eliminated at normal cell volume. This observation may shed light on previous controversial findings regarding the role of potassium in apoptosis (Kunzelmann, 2016; Model, 2014) and underscores the importance of cell volume in apoptotic signaling.

Cytoskeletal involvement is harder to definitively rule out due to the multiple elements that can be involved. Actin microfilaments are the major cytoskeletal components that serve as a scaffolding to support and organize other proteins. Many cytoskeleton-mediated events depend on the integrity of microfilaments, and depolymerization of actin by cytochalasin D is a standard method to check for the involvement of the cytoskeleton in signaling, including shrinkage-activated signaling (Korn and Korbmacher, 1999; Koltsova et al., 2008; Gastaldello et al., 2008). Generally, the cytoskeleton is an important player in apoptosis (Ndozangue-Touriguine et al., 2008) and, according to some data and theoretical considerations, may even be responsible for cell compression during the AVD (P.R. and M.A.M., in preparation). However, in this case we found no effect of cytochalasin D treatment on caspase activation, and must conclude that the cytoskeleton is not involved in shrinkage-mediated apoptotic signaling. Previous authors came to the same conclusion (Gastaldello et al., 2008).

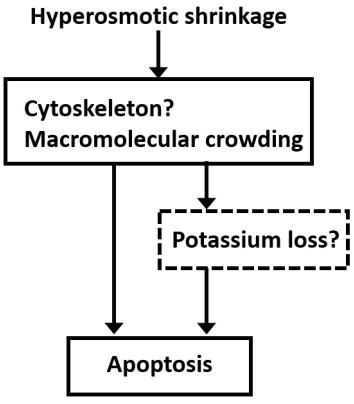

Fig. 8. The hypothesized signaling junctions in shrinkage-induced apoptosis. An increase in macromolecular crowding is the only inevitable consequence of hyperosmotic shrinkage. Changes in the cytoskeleton are possible but linked to shrinkage less directly. The loss of potassium can only be a more remote response. Of these factors, macromolecular crowding had the strongest impact on apoptosis in our experiments.

Having excluded the involvement of ion concentration and the cytoskeleton, macromolecular crowding appears the most plausible candidate for the role of an immediate shrinkage sensor and initial trigger of apoptosis in hyperosmotically shrunken cells. It is very likely that the AVD induced by other apoptotic factors has a similar stimulatory role in apoptosis. The range of phenomena in which macromolecular crowding may guide intracellular reactions must be much wider than is currently recognized. For example, we have previously argued that long-term adaptation to anisosmotic conditions must also be mediated by macromolecular crowding (Mudrak et al., 2018). After transferring HeLa cells from a 360 mOsm to a 440 mOsm medium, protein density kept increasing for the first hour but after 20 h returned to the initial level. There appears to be no other possible feedback mechanism than through protein density itself. Investigation of the effects of macromolecular crowding agents on cell-free apoptosis would be a promising next step.

MATERIALS AND METHODS

Chemicals, antibodies and plasmids

Valinomycin, nigericin, staurosporine and cytochalasin D were obtained from Cayman Chemicals (Ann Arbor, MI), and gramicidin and ouabain were from Sigma-Aldrich (St. Louis, MO). The ionophores (valinomycin, nigericin and gramicidin) were dissolved in ethanol at 200× the working concentration, ouabain in DMSO at 200× the working concentration, and cytochalasin D in DMSO at 5000× the working concentration and were stored at −20°C. We have verified that the solvents alone at their final concentrations had no effect on the cells. The apoptotic marker annexin V (FITC conjugate) was from Biolegend (San Diego, CA) and caspase-3 substrate NucView 488 was from Biotium (Fremont, CA). The following antibodies were used: mouse anti-cytochrome *c* (Biolegend; catalog number 612302, Lot B169559), goat anti-mouse–DyLight 488 (Thermo Fisher Scientific; catalog number 35503, Lot OJ92088) and AffiniPure anti-mouse–Cy3 from Jackson ImmunoResearch (West Grove, PA; catalog number 115-165-003, Lot 144931). The GFP–Bcl-2 plasmid was purchased from Addgene (Cambridge, MA; https://www.addgene.org/17999/).

Cell culture

HeLa and Madin–Darby canine kidney cells (MDCK) (all from ATCC, Manassas, VA; not authenticated recently) were grown in DMEM (Lonza) supplemented with 10% fetal bovine serum (FBS, Sigma-Aldrich) and antibiotics. For microscopic observation, cells were transferred no later than 24 h before the experiment either onto loose No. 1.5 coverslips kept in small cell culture dishes or to coverslip-bottom chambers (Thermo Fisher Scientific) precoated with 0.01% poly-L-Lysine or 0.01% collagen (both from Sigma-Aldrich). Cell cultures were maintained at 37°C in a humidified incubator in an atmosphere of 5% CO_2.

Cell treatment

Following the protocol described in Rana et al. (2019), intracellular monovalent ions were clamped by applying valinomycin, nigericin and gramicidin at 10 µM and ouabain at 0.5 mM. Incubation of cells with VNGO was carried out in solutions containing 150 mM of either KCl (for high-potassium buffer, HPB) or NaCl (for high-sodium buffer, HSB), 5.5 mM glucose, 1.25 mM $CaCl_2$, 1 mM $MgCl_2$, 5% FBS (which supplied an additional 7 mM NaCl) and 10 mM HEPES titrated to pH 7.3 with either KOH or NaOH to match the main cation of the medium. Variable concentrations of sucrose (Sigma-Aldrich), 0.4 µM cytochalasin D, or 2 µM of ST were also present in the incubation media where indicated. The duration of incubation was 8 h for HeLa and 4 h for MDCK cells.

Expression of GFP–Bcl-2

GFP–Bcl-2 was amplified in *E. coli* DH5α cells and extracted using a QIAGEN Maxi-prep kit. To prepare transfection reagent, DNA at a final concentration of 1 µg/ml was incubated with 3 µl of 1 mg/ml Lipofectamine 2000 (Invitrogen) in 100 µl of serum- and antibiotic-free DMEM for 20 min.

HeLa cells were plated 15 h before transfection at a density of 10^6 cells/cm^2 on coverslips placed in a 2 cm cell culture dish in complete growth medium. The DNA–lipofectamine complex was added to the cells at a 10% volume of the complete growth medium. Within 24 h, fluorescent Bcl-2 was expressed in the cells.

Apoptosis assays

Activated caspase-3 was visualized by incubation with 1 µM of NucView 488 for 10–15 min. Phosphatidylserine translocation was determined using an Annexin-V FITC apoptosis kit according to the manufacturer's protocol. Cytochrome *c* release from mitochondria was tested by immunostaining. Cells were fixed with 1% paraformaldehyde in PBS containing Mg^{2+} and Ca^{2+} for 20–30 min at room temperature. Next, the cells were permeabilized with 0.5% Triton in PBS with Mg^{2+} and Ca^{2+}, blocked with 5% goat serum, washed and stained with anti-cytochrome *c* antibody (1:500) for 3 h in PBS containing 1% goat serum, followed by goat anti-mouse-IgG–DyLight 488 at 1:5000 or AffiniPure anti-mouse IgG–Cy3 at 1:500 for two hours. For the last step, cell nuclei were stained using 1 µg/ml Hoechst for 20 min.

Microscopy and macromolecular density measurements

Fluorescence images of cytochrome *c* were taken on a Fluoview X1000 laser scanning confocal microscope (Olympus, Center Valley, PA) under 405 nm, 488 nm and 543 nm illumination using a 60×/1.42 oil-immersion objective. Caspase and annexin V-FITC fluorescent staining were visualized on an inverted IX81 microscope (Olympus) through FITC filters using a 20×/0.7 objective.

The volumes of HeLa cells were measured using the transmission-through-dye (TTD) method. Coverslips with attached HeLa cells were mounted on slides over spots made of silicone grease, leaving a gap approximately 30 µm deep, with cells facing the slide. The medium was first replaced with DMEM containing 7 mg/ml Acid Blue 9 (TCI America, Portland, OR) and a first set of transmission images was taken through a 630 nm bandpass filter. Because cells with intact membranes displace Acid Blue 9, the contrast in the transmission image quantitatively reflects cell thickness; image contrast can be converted into cell volume as described elsewhere (Model, 2015). To measure shrinkage induced by ionophores, the medium was replaced with either HPB or HSB containing VNGO, various concentrations of sucrose, and Acid Blue 9. The samples were kept at 37°C, and images of the same cells were taken at specified times.

At the same time, the total dry mass of the same cells was determined by the transport-of-intensity equation (TIE) method from two brightfield images mutually defocused by 5 µm and taken through a 485 nm bandpass filter (Mudrak et al., 2018). Because the TIE is based on the difference in refractive indices between the cell and the medium, and because the presence of sucrose in the medium raises its refractive index, a correction factor was applied, assuming the refractive index increment dn/dc=0.15 ml/g for sucrose and 0.19 ml/g for the average protein (Tumolo et al., 2004; Theisen, 2000). The ratio of dry mass to cell volume gives protein (or macromolecular, to be more precise) concentration averaged over cell volume. The MATLAB-based TIE code was provided by E. Schonbrun (Gorthi and Schonbrun, 2012).

Statistics

Data were analyzed by one-tailed homoscedastic *t*-test. Error bars in all the figures represent the standard error of the mean (s.e.m.).

Acknowledgements

We thank Ms Sandeep Kaur for help with plasmid preparation and Dr Souvik Dey who provided valuable advice. Drs A. Vereninov and F. Sachs made helpful suggestions on the manuscript.

Competing interests

The authors declare no competing or financial interests.

Author contributions

Conceptualization: M.A.M.; Methodology: P.S.R., M.K., M.A.M.; Validation: P.S.R.; Formal analysis: P.S.R.; Investigation: P.S.R., M.A.M.; Resources: P.S.R., M.K., M.A.M.; Writing - original draft: P.S.R., M.A.M.; Writing - review & editing: P.S.R., M.K., M.A.M.; Visualization: P.S.R., M.A.M.; Funding acquisition: M.K., M.A.M.

Funding

The research was supported by the Kent State University Research Council (M.A.M.) and by the Foundation for the National Institutes of Health, grants R03 CA230828 and R03 CA208384 (M.K.). Deposited in PMC for release after 12 months.

Peer review history

The peer review history is available online at https://jcs.biologists.org/lookup/doi/10.1242/jcs.243931.reviewer-comments.pdf

References

Abdalah, R., Wei, L., Francis, K. and Yu, S. P. (2006). Valinomycin-induced apoptosis in Chinese hamster ovary cells. *Neurosci. Lett.* **405**, 68-73. doi:10.1016/j.neulet.2006.06.055

Al-Habori, M. (2001). Macromolecular crowding and its role as intracellular signalling of cell volume regulation. *Int. J. Biochem. Cell Biol.* **33**, 844-864. doi:10.1016/S1357-2725(01)00058-9

Alfieri, R. R. and Petronini, P. G. (2007). Hyperosmotic stress response: comparison with other cellular stresses. *Pflügers Arch.* **454**, 173-185. doi:10.1007/s00424-006-0195-x

Bertrand, R., Solary, E., O'Connor, P., Kohn, K. W. and Pommier, Y. (1994). Induction of a common pathway of apoptosis by staurosporine. *Exp. Cell Res.* **211**, 314-321. doi:10.1006/excr.1994.1093

Bortner, C. D. and Cidlowski, J. A. (1996). Absence of volume regulatory mechanisms contributes to the rapid activation of apoptosis in thymocytes. *Am. J. Physiol.* **271**, C950-C961. doi:10.1152/ajpcell.1996.271.3.C950

Bortner, C. D. and Cidlowski, J. A. (1998). A necessary role for cell shrinkage in apoptosis. *Biochem. Pharmacol.* **56**, 1549-1559. doi:10.1016/S0006-2952(98)00225-1

Bortner, C. D. and Cidlowski, J. A. (2004). The role of apoptotic volume decrease and ionic homeostasis in the activation and repression of apoptosis. *Pflügers Arch.* **448**, 313-318. doi:10.1007/s00424-004-1266-5

Bortner, C. D., and Cidlowski, J. A. (2007). Cell shrinkage and monovalent cation fluxes: role in apoptosis. *Arch. Biochem. Biophys.* **462**, 176-188. doi:10.1016/j.abb.2007.01.020

Burg, M. B. (2000). Macromolecular crowding as a cell volume sensor. *Cell. Physiol. Biochem.* **10**, 251-256. doi:10.1159/000016371

Burg, M. B., Ferraris, J. D. and Dmitrieva, N. I. (2007). Cellular response to hyperosmotic stresses. *Physiol. Rev.* **87**, 1441-1474. doi:10.1152/physrev.00056.2006

Burgos, J. I., Morell, M., Mariángelo, J. I. E. and Vila Petroff, M. (2019). Hyperosmotic stress promotes endoplasmic reticulum stress-dependent apoptosis in adult rat cardiac myocytes. *Apoptosis* **24**, 785-797. doi:10.1007/s10495-019-01558-4

Colclasure, G. C. and Parker, J. C. (1991). Cytosolic protein concentration is the primary volume signal in dog red cells. *J. Gen. Physiol.* **98**, 881-892. doi:10.1085/jgp.98.5.881

Colclasure, G. C. and Parker, J. C. (1992). Cytosolic protein concentration is the primary volume signal for swelling-induced [K-Cl] cotransport in dog red cells. *J. Gen. Physiol.* **100**, 1-10. doi:10.1085/jgp.100.1.1

Criollo, A., Galluzzi, L., Maiuri, M. C., Tasdemir, E., Lavandero, S. and Kroemer, G. (2007). Mitochondrial control of cell death induced by hyperosmotic stress. *Apoptosis* **12**, 3-18. doi:10.1007/s10495-006-0328-x

David, J. M. and Rajasekaran, A. K. (2015). Gramicidin A: a new mission for an old antibiotic. *J. Kidney Cancer VHL* **2**, 15. doi:10.15586/jkcvhl.2015.21

Elmore, S. (2007). Apoptosis: a review of programmed cell death. *Toxicol. Pathol.* **35**, 495-516. doi:10.1080/01926230701320337

Ernest, N. J., Habela, C. W. and Sontheimer, H. (2008). Cytoplasmic condensation is both necessary and sufficient to induce apoptotic cell death. *J. Cell Sci.* **121**, 290-297. doi:10.1242/jcs.017343

Friis, M. B., Friborg, C. R., Schneider, L., Nielsen, M.-B., Lambert, I. H., Christensen, S. T. and Hoffmann, E. K. (2005). Cell shrinkage as a signal to apoptosis in NIH 3T3 fibroblasts. *J. Physiol.* **567**, 427-443. doi:10.1113/jphysiol.2005.087130

Fulton, A. B. (1982). How crowded is the cytoplasm? *Cell* **30**, 345-347. doi:10.1016/0092-8674(82)90231-8

Furlong, I. J., Mediavilla, C. L., Ascaso, R., Rivas, A. L. and Collins, M. K. L. (1998). Induction of apoptosis by valinomycin: mitochondrial permeability transition causes intracellular acidification. *Cell Death Differ.* **5**, 214-221. doi:10.1038/sj.cdd.4400335

Garner, M. M. and Burg, M. B. (1994). Macromolecular crowding and confinement in cells exposed to hypertonicity. *Am. J. Physiol.* **266**, C877-C892. doi:10.1152/ajpcell.1994.266.4.C877

Gastaldello, K., Husson, C., Dondeyne, J.-P., Vanherweghem, J.-L. and Tielemans, C. (2008). Cytotoxicity of mononuclear cells as induced by peritoneal dialysis fluids: insight into mechanisms that regulate osmotic stress-related apoptosis. *Perit. Dial. Int.* **28**, 655-666. doi:10.1177/089686080802800619

Ghosh, A., Keng, P. C. and Knauf, P. A. (2007). Hypertonicity induced apoptosis in HL-60 cells in the presence of intracellular potassium. *Apoptosis* **12**, 1281-1288. doi:10.1007/s10495-007-0054-z

Gnutt, D. and Ebbinghaus, S. (2016). The macromolecular crowding effect – from in vitro into the cell. *Biol. Chem.* **397**, 37-44. doi:10.1515/hsz-2015-0161

Gorthi, S. S. and Schonbrun, E. (2012). Phase imaging flow cytometry using a focus-stack collecting microscope. *Opt. Lett.* **37**, 707-709. doi:10.1364/OL.37.000707

Hoffmann, E. K. and Pedersen, S. F. (2011). Cell volume homeostatic mechanisms: effectors and signalling pathways. *Acta Physiol. (Oxf.)* **202**, 465-485. doi:10.1111/j.1748-1716.2010.02190.x

Hoffmann, E. K., Lambert, I. H. and Pedersen, S. F. (2009). Physiology of cell volume regulation in vertebrates. *Physiol. Rev.* **89**, 193-277. doi:10.1152/physrev.00037.2007

Horio, M., Ito, A., Matsuoka, Y., Moriyama, T., Orita, Y., Takenaka, M. and Imai, E. (2001). Apoptosis induced by hypertonicity in Madin Darley canine kidney cells: protective effect of betaine. *Nephrol. Dial. Transplant.* **16**, 483-490. doi:10.1093/ndt/16.3.483

Inai, Y., Yabuki, M., Kanno, T., Akiyama, J., Yasuda, T. and Utsumi, K. (1997). Valinomycin induces apoptosis of ascites hepatoma cells (AH-130) in relation to mitochondrial membrane potential. *Cell Struct. Funct.* **22**, 555-563. doi:10.1247/csf.22.555

Janmey, P. A. and Kinnunen, P. K. J. (2006). Biophysical properties of lipids and dynamic membranes. *Trends Cell Biol.* **16**, 538-546. doi:10.1016/j.tcb.2006.08.009

Klimanova, E. A., Sidorenko, S. V., Tverskoi, A. M., Shiyan, A. A., Smolyaninova, L. V., Kapilevich, L. V., Gusakova, S. V., Maksimov, G. V., Lopina, O. D. and Orlov, S. N. (2019). Search for intracellular sensors involved in the functioning of monovalent cations as secondary messengers. *Biochemistry (Mosc.)* **84**, 1280-1295. doi:10.1134/S0006297919110063

Koch, J.-P. and Korbmacher, C. (1999). Osmotic shrinkage activates nonselective cation (NSC) channels in various cell types. *J. Membr. Biol.* **168**, 131-139. doi:10.1007/s002329900503

Koh, J.-Y., Wie, M. B., Gwag, B. J., Sensi, S. L., Canzoniero, L. M. T., Demaro, J., Csernansky, C. and Choi, D. W. (1995). Staurosporine-induced neuronal apoptosis. *Exp. Neurol.* **135**, 153-159. doi:10.1006/exnr.1995.1074

Koivusalo, M., Kapus, A. and Grinstein, S. (2009). Sensors, transducers, and effectors that regulate cell size and shape. *J. Biol. Chem.* **284**, 6595-6599. doi:10.1074/jbc.R800049200

Koltsova, S. V., Gusakova, S. V., Anfinogenova, Y. J., Baskakov, M. B. and Orlov, S. N. (2008). Vascular smooth muscle contraction evoked by cell volume modulation: role of the cytoskeleton network. *Cell. Physiol. Biochem.* **21**, 029-036. doi:10.1159/000113744

Kunzelmann, K. (2016). Ion channels in regulated cell death. *Cell. Mol. Life Sci.* **73**, 2387-2403. doi:10.1007/s00018-016-2208-z

Luo, L., Li, D.-Q. and Pflugfelder, S. C. (2007). Hyperosmolarity-induced apoptosis in human corneal epithelial cells is mediated by cytochrome c and MAPK pathways. *Cornea* **26**, 452-460. doi:10.1097/ICO.0b013e318030d259

Maeno, E., Shimizu, T. and Okada, Y. (2006a). Normotonic cell shrinkage induces apoptosis under extracellular low Cl- conditions in human lymphoid and epithelial cells. *Acta Physiol. (Oxf.)* **187**, 217-222. doi:10.1111/j.1748-1716.2006.01554.x

Maeno, E., Takahashi, N. and Okada, Y. (2006b). Dysfunction of regulatory volume increase is a key component of apoptosis. *FEBS Lett.* **580**, 6513-6517. doi:10.1016/j.febslet.2006.10.074

Marshall, W. F. (2016). Cell geometry: how cells count and measure size. *Annu. Rev. Biophys.* **45**, 49-64. doi:10.1146/annurev-biophys-062215-010905

Michea, L., Ferguson, D. R., Peters, E. M., Andrews, P. M., Kirby, M. R. and Burg, M. B. (2000). Cell cycle delay and apoptosis are induced by high salt and urea in renal medullary cells. *Am. J. Physiol. Renal Physiol.* **278**, F209-F218. doi:10.1152/ajprenal.2000.278.2.F209

Minton, A. P. (2001). The influence of macromolecular crowding and macromolecular confinement on biochemical reactions in physiological media. *J. Biol. Chem.* **276**, 10577-10580. doi:10.1074/jbc.R100005200

Mittal, S., Chowhan, R. K. and Singh, L. R. (2015). Macromolecular crowding: macromolecules friend or foe. *Biochim. Biophys. Acta* **1850**, 1822-1831. doi:10.1016/j.bbagen.2015.05.002

Model, M. A. (2014). Possible causes of apoptotic volume decrease: an attempt at quantitative review. *Am. J. Physiol.* **306**, C417-C424. doi:10.1152/ajpcell.00328.2013

Model, M. A. (2015). Cell volume measurements by optical transmission microscopy. *Curr. Protoc. Cytom.* **72**, 12.39.1-12.39.9. doi:10.1002/0471142956.cy1239s72

Model, M. A., Mudrak, N. J., Rana, P. S. and Clements, R. J. (2018). Staurosporine-induced apoptotic water loss is cell- and attachment-specific. *Apoptosis* **23**, 449-455. doi:10.1007/s10495-018-1471-x

Mongin, A. A. and Orlov, S. N. (2001). Mechanisms of cell volume regulation and possible nature of the cell volume sensor. *Pathophysiology* **8**, 77-88. doi:10.1016/S0928-4680(01)00074-8

Mourão, M. A., Hakim, J. B. and Schnell, S. (2014). Connecting the dots: the effects of macromolecular crowding on cell physiology. *Biophys. J.* **107**, 2761-2766. doi:10.1016/j.bpj.2014.10.051

Mudrak, N. J., Rana, P. S. and Model, M. A. (2018). Calibrated brightfield-based imaging for measuring intracellular protein concentration. *Cytometry A* **93**, 297-304. doi:10.1002/cyto.a.23145

Ndozangue-Touriguine, O., Hamelin, J. and Bréard, J. (2008). Cytoskeleton and apoptosis. *Biochem. Pharmacol.* **76**, 11-18. doi:10.1016/j.bcp.2008.03.016

Orlov, S. N. and Hamet, P. (2006). Intracellular monovalent ions as second messengers. *J. Membr. Biol.* **210**, 161-172. doi:10.1007/s00232-006-0857-9

Orlov, S. N., Shiyan, A., Boudreault, F., Ponomarchuk, O. and Grygorczyk, R. (2018). Search for upstream cell volume sensors. The role of plasma membrane and cytoplasmic hydrogel. *Curr. Top. Membr.* **81**, 53-82. doi:10.1016/bs.ctm.2018.07.001

Papakonstanti, E. A., Vardaki, E. A. and Stournaras, C. (2000). Actin cytoskeleton: a signaling sensor in cell volume regulation. *Cell. Physiol. Biochem.* **10**, 257-264. doi:10.1159/000016366

Park, I. S. and Kim, J. E. (2002). Potassium efflux during apoptosis. *J. Biochem. Mol. Biol.* **35**, 41-46. doi:10.5483/BMBRep.2002.35.1.041

Pedersen, S. F., Hoffmann, E. K. and Mills, J. W. (2001). The cytoskeleton and cell volume regulation. *Comp. Biochem. Physiol. A Mol. Integr. Physiol.* **130**, 385-399. doi:10.1016/S1095-6433(01)00429-9

Pedersen, S. F., Kapus, A. and Hoffmann, E. K. (2011). Osmosensory mechanisms in cellular and systemic volume regulation. *J. Am. Soc. Nephrol.* **22**, 1587-1597. doi:10.1681/ASN.2010121284

Rana, P. S., Gibbons, B. A., Vereninov, A. A., Yurinskaya, V. E., Clements, R. J., Model, T. A. and Model, M. A. (2019). Calibration and characterization of intracellular Asante Potassium Green probes, APG-2 and APG-4. *Anal. Biochem.* **567**, 8-13. doi:10.1016/j.ab.2018.11.024

Shimizu, T., Maeno, E. and Okada, Y. (2007). Prerequisite role of persistent cell shrinkage in apoptosis of human epithelial cells. *Sheng Li Xue Bao* **59**, 512-516.

Strange, K., Yamada, T. and Denton, J. S. (2019). A 30-year journey from volume-regulated anion currents to molecular structure of the LRRC8 channel. *J. Gen. Physiol.* **151**, 100-117. doi:10.1085/jgp.201812138

Theisen, A. (2000). *Refractive Increment Data-Book for Polymer and Biomolecular Scientists*: Nottingham University Press.

Tumolo, T., Angnes, L. and Baptista, M. S. (2004). Determination of the refractive index increment (dn/dc) of molecule and macromolecule solutions by surface plasmon resonance. *Anal. Biochem.* **333**, 273-279. doi:10.1016/j.ab.2004.06.010

Yu, S. P. (2003). Regulation and critical role of potassium homeostasis in apoptosis. *Prog. Neurobiol.* **70**, 363-386. doi:10.1016/S0301-0082(03)00090-X

Yu, S. P., Canzoniero, L. M. T. and Choi, D. W. (2001). Ion homeostasis and apoptosis. *Curr. Opin. Cell Biol.* **13**, 405-411. doi:10.1016/S0955-0674(00)00228-3

Zhou, H.-X., Rivas, G. and Minton, A. P. (2008). Macromolecular crowding and confinement: biochemical, biophysical, and potential physiological consequences. *Annu. Rev. Biophys.* **37**, 375-397. doi:10.1146/annurev.biophys.37.032807.125817

Zigmond, S. H. (1996). Signal transduction and actin filament organization. *Curr. Opin. Cell Biol.* **8**, 66-73. doi:10.1016/S0955-0674(96)80050-0